marine drugs

MDPI

Article

New Cembranoids and a Biscembranoid Peroxide from the Soft Coral *Sarcophyton cherbonnieri*

Chia-Chi Peng [1], Chiung-Yao Huang [1], Atallah F. Ahmed [2,3], Tsong-Long Hwang [4,5,6], Chang-Feng Dai [7] and Jyh-Horng Sheu [1,8,9,*]

1 Department of Marine Biotechnology and Resources, National Sun Yat-sen University, Kaohsiung 804, Taiwan; m045020008@student.nsysu.edu.tw (C.-C.P.); huangcy@mail.nsysu.edu.tw (C.-Y.H.)
2 Department of Pharmacognosy, College of Pharmacy, King Saud University, Riyadh 11451, Saudi Arabia; afahmed@ksu.edu.sa
3 Department of Pharmacognosy, Faculty of Pharmacy, Mansoura University, Mansoura 35516, Egypt
4 Graduate Institute of Natural Products, College of Medicine, Chang Gung University, Taoyuan 333, Taiwan; htl@mail.cgu.edu.tw
5 Research Center for Industry of Human Ecology and Graduate Institute of Health Industry Technology, Chang Gung University of Science and Technology, Taoyuan 333, Taiwan
6 Department of Anesthesiology, Chang Gung Memorial Hospital, Taoyuan 333, Taiwan
7 Institute of Oceanography, National Taiwan University, Taipei 112, Taiwan; corallab@ntu.edu.tw
8 Graduate Institute of Natural Products, Kaohsiung Medical University, Kaohsiung 807, Taiwan
9 Frontier Center for Ocean Science and Technology, National Sun Yat-sen University, Kaohsiung 804, Taiwan
* Correspondence: sheu@mail.nsysu.edu.tw; Tel.: +886-7-525-2000 (ext. 5030); Fax: +886-7-525-5020

Received: 27 June 2018; Accepted: 31 July 2018; Published: 6 August 2018

Abstract: Six new cembranoids, cherbonolides A−E (**1**–**5**) and bischerbolide peroxide (**6**), along with one known cembranoid, isosarcophine (**7**), were isolated from the Formosan soft coral *Sarcophyton cherbonnieri*. The structures of these compounds were elucidated by detailed spectroscopic analysis and chemical methods. Compound **6** was discovered to be the first example of a molecular skeleton formed from two cembranoids connected by a peroxide group. Compounds **1**–**7** were shown to have the ability of inhibiting the production of superoxide anions and elastase release in *N*-formyl-methionyl-leucyl-phenyl-alanine/cytochalasin B (fMLF/CB)-induced human neutrophils.

Keywords: *Sarcophyton cherbonnieri*; cembranoid; biscembranoid peroxide; anti-inflammatory activity; elastase release inhibition

1. Introduction

Many cembrane-based natural products have been shown to exhibit significant activities such as cytotoxicity [1–14] and anti-inflammatory activity [9,11,13–18]. From the experience of searching bioactive metabolites from soft corals, series of cembranoids have been unveiled from octocorals (Alcyonaceae) belonging to the genera *Sarcophyton*, [1–8,16], *Sinularia* [9–12,17,18] and *Lobophyton* [13–15]. Also, previous studies showed that two cembranoid units could form biscembranoid-type compounds by Diels-Alder reaction [19–21], radical dimerization [22,23], or connection with a sulfur atom [18], making the chemistry of cembranes more complex and interesting than monomeric form.

Our current chemical investigation on *Sarcophyton cherbonnieri* led to the discovery of six new cembranoids—cherbonolides A−E (**1**–**5**) and bischerbolide peroxide (**6**)—and one known compound, isosarcophine (**7**) [24]. The structures of **1**–**7** (Figure 1) were elucidated by extensive spectroscopic analysis, including detailed 2D nuclear magnetic resonance (NMR) experiments and chemical methods. Compounds **2**, **5**, and **6** were characterized as cembranoids bearing an allylic peroxyl group as those

previously discovered marine cembranoidal peroxides [25–29]. Furthermore, compound **6** is the first example of a biscembranoid with two cembranoidal units interconnected by a peroxyl group. The absolute configurations of **1** and **3** were further established using a modified Mosher's reaction. Also, evaluation of the in vitro anti-inflammatory activities through the inhibition of superoxide anion ($O_2^{-\bullet}$) generation and elastase release in *N*-formyl-methionyl-leucyl-phenyl-alanine/cytochalasin B (fMLF/CB)-induced human neutrophils was carried out.

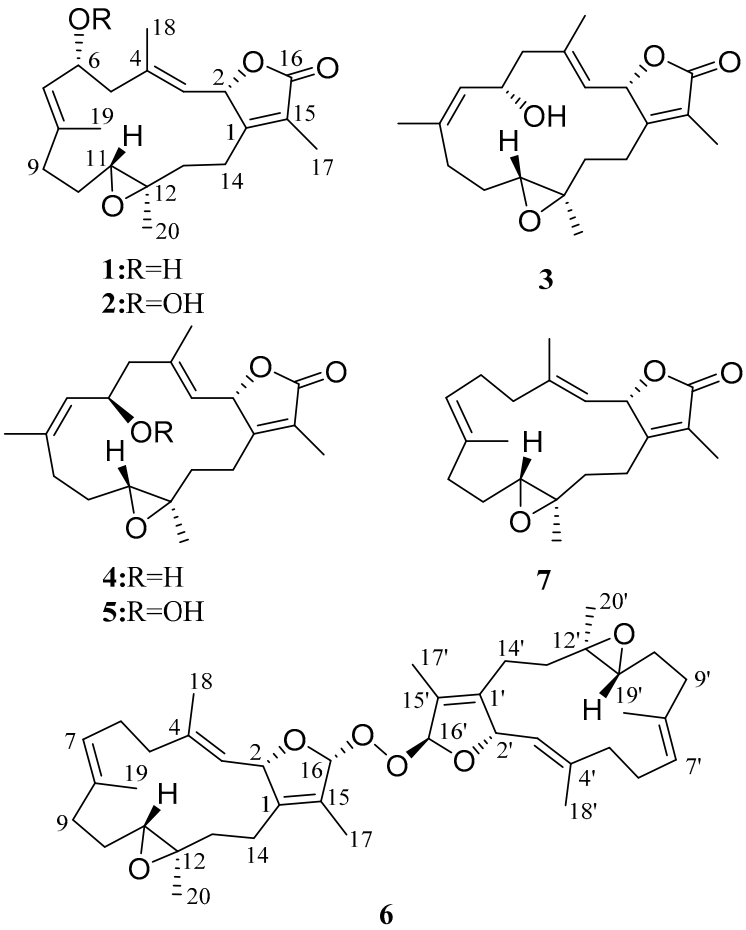

Figure 1. Cembranoid isolated from *Sarcophyton cherbonnieri.*

2. Results and Discussion

The soft coral *S. cherbonnieri* (1.2 kg, wet weight) was collected using SCUBA diving from Jihui Port of Taitung, Taiwan, in March 2013, and stored in a freezer before extraction. The freeze-dried organisms (207 g) were sliced into small pieces, followed by exhaustive extraction with ethyl acetate (EtOAc). The EtOAc extract was dried with anhydrous sodium sulfate (Na_2SO_4). After removal of EtOAc under reduced pressure, the residue yielded was separated by silica gel column chromatography and the resolved fractions were further purified by reverse-phase C_{18} high-performance liquid chromatography (HPLC) to afford compounds **1**–**7** (Figure 1), the structures of which were elucidated on the basis of spectroscopic analyses (Supplementary Materials, Figures S1–S46).

Cherbonolide A (**1**) was isolated as a colorless oil. The molecular formula $C_{20}H_{28}O_4$ of **1** was determined by the high-resolution electrospray ionization mass spectrometry (HRESIMS) (*m*/*z* calcd 355.1880; found 355.1879, $[M + Na]^+$), which required seven degrees of unsaturation. The IR spectrum of **1** showed the presence of a hydroxyl group (ν_{max} 3457 cm^{-1}) and a lactonic carbonyl group (ν_{max} 1746 cm^{-1}). The presence of 20 carbons in the structure of **1**, including four methyls, five sp^3 methylenes, three sp^3 oxygenated methines, two sp^2 methines, one sp^3 and five sp^2 nonprotoned carbon atoms were

assigned with the aid of distortionless enhancement by polarization transfer (DEPT) spectra. The NMR peaks resonating at δ_C 174.4 (C), 160.7 (C), 123.8 (C), 77.8 (CH) and 8.8 (CH_3), and δ_H 5.44 (1H, dd, J = 10.0, 1.6 Hz) and δ_H 1.86 (3H, s), are characteristic signals of an α-methyl-α,β-unsaturated-γ-lactone ring by comparison of the NMR data of the γ-lactone ring of known compound isosarcophine (**7**). Signals at δ_C 60.8 (C), 61.4 (CH) and δ_H 2.42 (1H, dd, J = 10.8, 2.8 Hz) showed the presence of a trisubstituted epoxide. Two trisubstituted double bonds could also be identified by NMR signals resonating at δ_C 122.2 (CH), δ_C 141.6 (C) and δ_H 4.90 (1H, d, J = 10.0 Hz), and at δ_C 128.1 (CH), δ_C 139.8 (C) and δ_H 5.20 (1H, d, J = 10.4 Hz), respectively. The correlations identified from the ^{1}H-^{1}H correlation spectroscopy (^{1}H-^{1}H COSY) spectrum revealed four separate proton sequences, as shown in Figure 2, which were assembled by heteronuclear multiple bond correlation (HMBC) correlations (Figure 2). Key HMBC correlations of H-2 (δ_H 5.44, 1H, dd, J = 10.0, 1.6 Hz) to C-1; H_2-14 (δ_H 2.01, m)/C-1; H_3-17 (δ_H 1.86, s) to C-1, C-15 and C-16; H_3-18 (δ_H 1.70, s) to C-3, C-4 and C-5; H_3-19 (δ_H 1.86, s) to C-7, C-8 and C-9; and H_3-20 (δ_H 1.33, s) to C-11, C-12 and C-13, established the connection of the four proton sequences, and thus constructed the 14-membered ring carbon skeleton, which also indicated the presence of a hydroxyl at C-6. Thus, the planar structure of **1** was established.

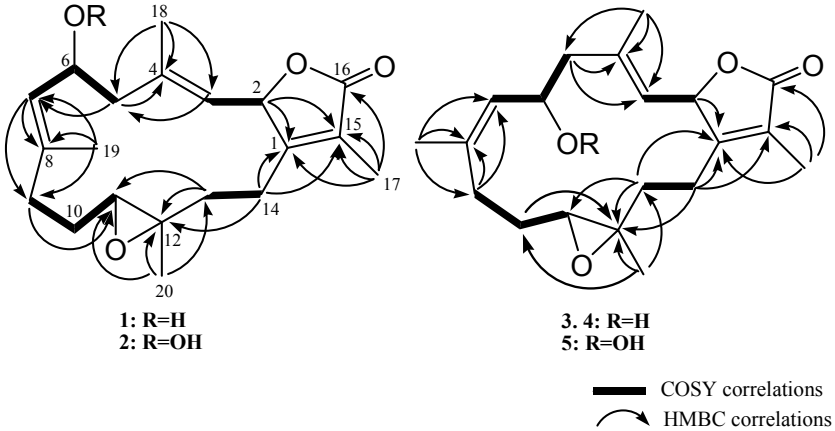

Figure 2. Selected ^{1}H-^{1}H COSY and HMBC correlations of **1**, **2** and **3**−**5**.

Further, careful analysis of nuclear Overhauser enhancement (NOE) correlations was applied to establish the relative stereochemistry of **1**, as shown in Figure 3. The NOE spectrum revealed that H-2 (δ_H 5.44, dd, J = 10.0, 1.6 Hz) showed NOE correction with H_3-18 (δ_H 1.70, s); therefore, assuming a β-orientation of H-2, H_3-18 should be β-oriented, too. Moreover, H_3-18 exhibited NOE correlation with H-6 (δ_H 4.70, ddd, J = 10.4, 10.4, 5.2 Hz), revealing the β-orientation of H-6 and the R* configuration of C-6. One methylene proton at C-13 exhibited NOE correlation with H-2 and was characterized as H-13β (δ_H 1.06, m), while the other proton was assigned as H-13α (δ_H 2.03, m). NOE correlations of H-13β with H-11 (δ_H 2.42, dd, J = 10.8, 2.8 Hz) and H-13α with H_3-20 (δ_H 1.33, s) reflected the β-orientation of H-11 and the α-orientation of H_3-20, and hence the R* configurations of both C-11 and C-12. The E geometries of the trisubstituted C-3/C-4 and C-7/C-8 double bonds were also assigned from the NOE correlations of H_3-18 (δ_H 1.70, s) with H-2, but not with H-3 (δ_H 4.90, d, J = 10.0 Hz), as well as H_3-19 (δ_H 1.86, s) with H-6, but not with H-7 (δ_H 5.20, d, J = 10.4 Hz), and were also confirmed by the upfield chemical shifts (δ_C < 20 ppm) observed for both C-18 (δ_C 15.9) and C-19 (δ_C 14.9) [30]. Based on the above observations and the detailed analysis of other NOE correlations, the relative configuration of this compound was established. Furthermore, the absolute configuration of **1** at C-6 was determined by the modified Mosher's esterification method [31,32]. The (S)- and (R)-MTPA esters of **1** (**1a** and **1b**, respectively, as shown in Figure 4) were afforded by the reaction of **1** with (R)-(-) and (S)-(+)-MTPA chloride, respectively. Determination of the Δδ values (δ_S−δ_R) for protons nearing C-6 resulted in the establishment of the R configuration at C-6 in **1** (Figure 4). The absolute configuration of **1** was

thus assigned as 2*S*,6*R*,11*R*,12*R*, mostly the same as that of isosarcophine (**7**) [24], except that of C-6. Therefore, cherbonolide A (**1**) was identified as 6-*α*-hydroxyisosarcophine.

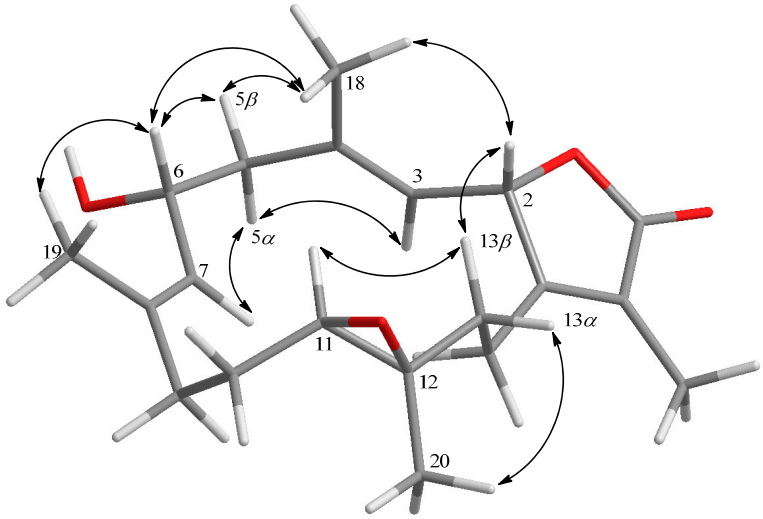

Figure 3. Key NOESY correlations of **1**.

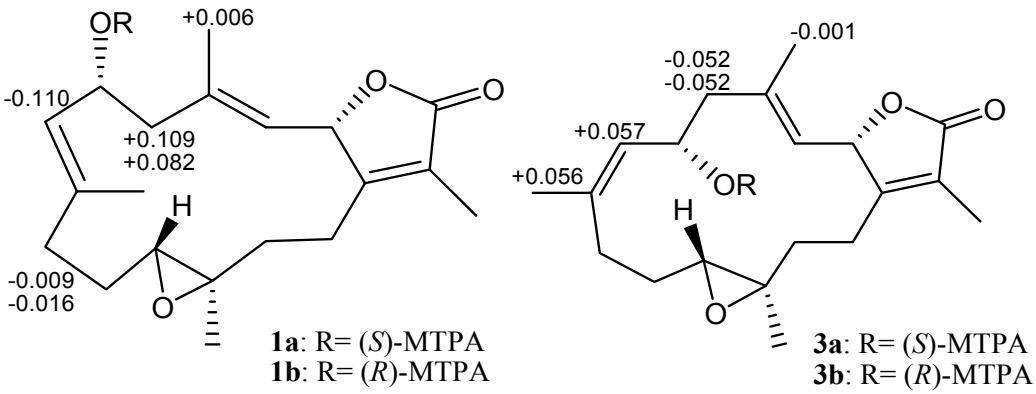

Figure 4. ^{1}H NMR chemical shift differences Δδ ($\delta_S - \delta_R$) in ppm for the MTPA esters of **1** and **3**.

The molecular formula of cherbonolide B (**2**) was determined to be $C_{20}H_{28}O_5$ by the HRESIMS (*m*/*z* calcd 371.1830; found 371.1829, $[M + Na]^+$), having one more oxygen than 1. Moreover, both **1** and **2** had almost identical ^{1}H and ^{13}C NMR data (Table 1), except for those of C-6. The allylic hydroxy group of **1** at C-6 was substituted by a hydroperoxyl in **2**, with the characteristic signal of a broad singlet in the downfield region, δ_H 7.99 [26,33,34]. Obvious downfield shifts of C-6 (δ_C 65.2 in **1**, 78.3 in **2**) and H-6 (δ_H 4.70 in **1**, 4.97 in **2**) were also observed, indicating that **2** possesses the hydroperoxy group at C-6. Furthermore, reduction of **2** by reaction with triphenylphosphine afforded **1**. On the basis of the above analyses, the planar structure and the (2*S*,6*R*,11*R*,12*R*)-configuration of **2** were determined.

Table 1. ^{1}H and ^{13}C NMR chemical shifts for compounds **1**–**4**.

Position	1		2		3		4	
	δ_H, m (*J* in Hz) [a]	δ_C [b], type	δ_H, m (*J* in Hz) [a]	δ_C [b], type	δ_H, m (*J* in Hz) [c]	δ_C [d], type	δ_H, m (*J* in Hz) [c]	δ_C [d], type
1		160.7, C		160.6, C		160.6, C		159.8, C
2	5.44, dd (10.0, 1.6)	77.8, CH	5.43, dd (10.0, 1.6)	77.8, CH	4.91, dd (10.0, 1.6)	78.4, CH	4.98, d (10.4)	77.8, CH
3	4.90, d (10.0)	122.2, CH	4.91, d (10.0)	122.7, CH	4.55, d (10.0)	123.9, CH	4.45, d (10.4)	123.5, CH
4		141.6, C		140.8, C		140.2, C		139.4, C
5α	2.20, m	47.9, CH_2	2.18, dd (12.4, 10.8)	42.6, CH_2	2.42, dd (12.0, 3.2)	49.1, CH_2	1.98, m	49.3, CH_2
5β	2.76, dd (12.8, 5.2)		2.87, dd (12.4, 4.4)		189, m		2.25, dd (12.8, 3.6)	
6	4.70, ddd (10.4, 10.4, 5.2)	65.2, CH	4.97, ddd (10.8, 9.2, 4.4)	78.3, CH	3.84, dd (9.2, 9.2)	69.6, CH	4.21, ddd (11.2, 9.2, 3.6)	64.8, CH
7	5.20, d (10.4)	128.1, CH	5.05, d (9.2)	123.1, CH	5.09, d (9.2)	131.6, CH	4.84, d (9.2)	131.2, CH
8		139.8, C		144.2, C		138.4, C		139.4, C
9α	2.03, m	36.8, CH_2	2.07, m	36.9, CH_2	2.21, ddd (13.6, 13.6, 2.4)	28.2, CH_2	1.58, m	28.5, CH_2
9β	2.38, m		2.42, m		1.63, m		2.30, dd (13.2, 4.8)	
10α	1.29, m	23.5, CH_2	1.35, m	23.6, CH_2	1.16, m	23.9, CH_2	1.60, m	22.7, CH_2
10β	2.51, m		2.17, m		1.84, m		1.28, m	
11	2.42, dd (10.8, 2.8)	61.4, CH	2.43, m	61.4, CH	2.24, dd (10.4, 2.4)	58.9, CH	1.98, m	62.6, CH
12		60.8, C		60.8, C		59.7, CH		60.9, C
13α	2.03, m	36.9, CH_2	2.02, m	37.0, CH_2	1.49, m	35.5, CH_2	1.61, m	37.1, CH_2
13β	1.06, m		1.07, m		0.98, m		0.65, m	
14α	2.49, m	23.7, CH_2	2.52, m	23.7, CH_2	1.58, m	22.2, CH_2	2.08, m	23.1, CH_2
14β	2.01, m		2.03, m		1.58, m		1.65, m	
15		123.8, C		123.8, C		123.8, C		123.7, C
16		174.4, C		174.4, C		173.9, C		174.3, C
17	1.86, s	8.8, CH_3	1.86, s	8.7, CH_3	1.64, s	8.8, CH_3	1.63, s	8.8, CH_3
18	1.70, s	15.9, CH_3	1.72, s	15.9, CH_3	1.31, s	18.1, CH_3	1.28, s	16.9, CH_3
19	1.86, s	14.9, CH_3	1.89, s	15.3, CH_3	1.45, s	22.2, CH_3	1.32, s	21.8, CH_3
20	1.33, s	15.8, CH_3	1.33, s	15.8, CH_3	1.00, s	17.1, CH_3	0.99, s	16.4, CH_3
6-OOH			7.99, br s					

[a] Spectrum recorded at 400 MHz in $CDCl_3$. [b] Spectrum recorded at 100 MHz in $CDCl_3$. [c] Spectrum recorded at 400 MHz in C_6D_6. [d] Spectrum recorded at 100 MHz in C_6D_6.

Cherbonolide C (**3**) should have the same molecular formula as **1**, according to HRESIMS data. Also, the ^{1}H-^{1}H COSY and HMBC correlations (Figure 2) of **3** are similar to those of **1**, suggesting that these compounds possess almost the same molecular skeleton. Analysis of NOE correlations (Figure 5) showed that the relative configurations at C-2, C-11 and C-12 in **1** and **3** are the same. Assuming the β-orientation of H-2, as H_3-18 showed NOE interaction with H-2 but not with H-3, the *E* geometry was assigned to the trisubstituted C-3/C-4 double bond. One of the methylene protons at C-5 (δ_H 2.42, dd, J = 12.0, 3.2 Hz) displayed NOE interaction with H-3, but not with H_3-18, and was hence determined as H-5α. Further, H-6 (δ_H 3.84, dd, J = 9.2, 9.2 Hz) showed NOE correlations with H-5α and H-9α, but not with H-9β and H_3-19. These observations, together with NOE correlations of H-9β/H_3-19, H_3-19/H-7 and H-7/H_3-18, enabled deduction of the α-orientation of H-6 and led to the assignment of a 6*S** configuration and a *Z* geometry of the trisubstituted C-7/C-8 double bond in **3**. The olefinic methyl group attaching at C-8 showed carbon signal at δ_C 22.2 ppm further confirmed the *Z* geometry of C-7/C-8 double bond [30]. The absolute configuration of **3** at C-6 was also verified by using the modified Mosher's method. Determination of the Δδ values ($\delta_S - \delta_R$, shown in Figure 4) for protons neighboring C-6 further confirmed the *S* configuration at C-6 in **3** (Figure 4). The absolute configuration of **3** was thus assigned as 2*S*,6*S*,11*R* and 12*R*. Thus, cherbonolide C (**3**) is the 7*Z* isomer of cherbonolide A (**1**).

Cherbonolide D (**4**) was found to be an isomer of **3** according to HRESIMS. Both compounds have almost the same ^{1}H-^{1}H COSY and HMBC correlations, indicating they have the same molecular skeleton. NMR data of **3** and **4** are nearly the same (Table 1), except for those of CH-6, suggesting that **4** could be the C-6 epimer of **3**. The (2*S*,6*R*,11*R*,12*R*)-configuration and the *E* and *Z* geometries of C-3/C-4 and C-7/C-8 double bonds of **4**, respectively, were also established by analysis of NOE correlations to be as those of **3** (Figure 5).

Cherbonolide E (**5**) was determined to have a molecular formula $C_{20}H_{28}O_5$ from its HRESIMS data (m/z calcd 371.1830; found 371.1829, $[M + Na]^+$), with one more oxygen than in **4**. Compounds **4** and **5** displayed almost identical ^{1}H and ^{13}C NMR data (Table 2), except for those of CH-6. It was found that the hydroxy substituent of **4** at C-6 was replaced by a hydroperoxy group in **5**, with the characteristic signal of a broad singlet at δ_H 7.25 [26,33,34]. The obvious downfield shifts of C-6 (δ_C 64.8 in **4**, 78.9 in **5**) and H-6 (δ_H 4.21 in **4**, 4.58 in **5**) also confirmed the substitution of a hydroperoxy group at C-6 of **5**. Furthermore, reduction of **5** with triphenylphosphine could afford **4**. Therefore, the structure of **5**, with the (2*S*,6*R*,11*R*,12*R*)-configuration, was determined.

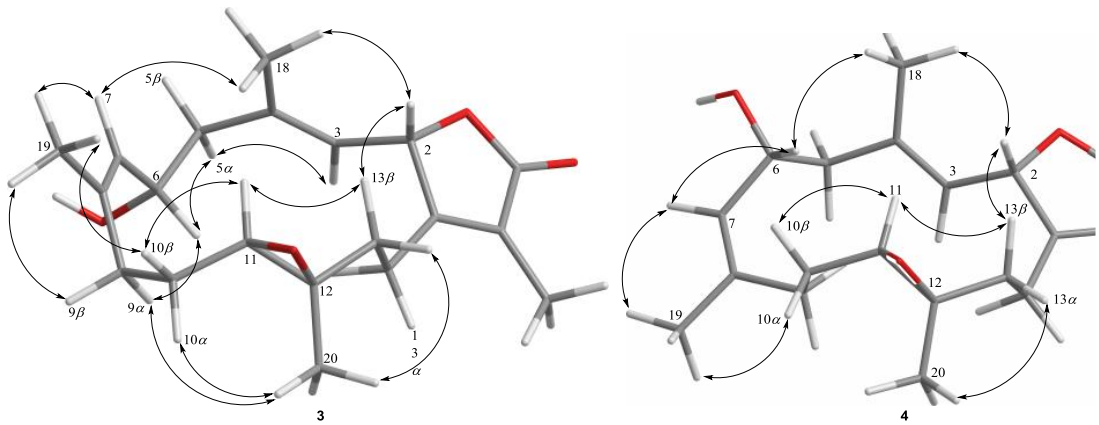

Figure 5. Key NOESY correlations for **3** and **4**.

Table 2. ^{1}H and ^{13}C NMR chemical shifts for compounds **5** and **6**.

Position	5				6		
	δ_H, m (*J* in Hz) [a]	δ_C [b], type	δ_H, m (*J* in Hz) [c]	δ_C [d], type		δ_H, m (*J* in Hz) [c]	δ_C [d], type
1		160.4, C		141.4, C	1′		141.5, C
2	4.95, d (10.0)	78.4, CH	5.28, d (10.0)	82.7, CH	2′	5.50, d (10.0)	81.9, CH
3	4.42, d (10.0)	124.6, CH	5.06, d (10.0)	126.4, CH	3′	4.92, d (10.0)	125.1, CH
4		139.2, C		140.2, C	4′		141.0, C
5α	1.95, m	44.6, CH_2	2.21, m	38.5, CH_2	5′α	2.21, m	38.8, CH_2
5β	2.47, br d (11.0)		2.32, m		5′β	2.31, m	
6	4.58, ddd (11.0, 9.5, 2.5)	78.9, CH		24.2, CH_2	6′		24.2, CH_2
6α			2.07, m		6′α	2.07, m	
6β			2.42, m		6′β	2.42, m	
7	4.78, d (9.5)	126.6, CH	4.98, dd (9.2, 9.2)	125.6, CH	7′	4.95, dd (9.2, 9.2)	125.5, CH
8		143.8, C		133.1, C	8′		133.3, C
9α	1.65, m	29.8, CH_2	1.96, m	36.6, CH_2	9′α	1.96, m	36.6, CH_2
9β	2.52, dd (14.0, 4.5)		2.27, m		9′β	2.27, m	
10α	1.28, m	23.4, CH_2	1.22, m	23.6, CH_2	10′α	1.22, m	23.7, CH_2
10β	1.62, m		2.04, m		10′β	2.04, m	
11	1.97, m	63.3, CH	2.51, m	62.1, CH	11′	2.51, m	62.2, CH
12		61.5, C		61.2, CH	12′		61.3, C
13α	1.59, m	37.6, CH_2	1.83, m	37.3, CH_2	13′α	1.83, m	37.4, CH_2
13β	0.64, m		0.95, m		13′β	0.95, m	
14α	2.07, m	23.7, CH_2	2.33, m	22.6, CH_2	14′α	2.33, m	22.7, CH_2
14β	1.61, m		1.81, m		14′β	1.81, m	
15		124.3, C		124.9, C	15′		124.9, C
16		174.3, C	6.13, br s	114.3, C	16′	6.17, d (3.6)	114.4, CH
17	1.63, s	9.4, CH_3	1.72, s	10.2, CH_3	17′	1.73, s	10.2, CH_3
18	1.29, s	17.3, CH_3	1.58, s	14.6, CH_3	18′	1.59, s	14.6, CH_3
19	1.34, s	22.5, CH_3	1.65, s	14.7, CH_3	19′	1.65, s	14.7, CH_3
20	0.98, s	16.9, CH_3	1.27, s	15.7, CH_3	20′	1.27, s	15.7, CH_3
6-OOH	7.25, br s						

[a] Spectrum recorded at 500 MHz in C_6D_6. [b] Spectrum recorded at 125 MHz in C_6D_6. [c] Spectrum recorded at 400 MHz in $CDCl_3$. [d] Spectrum recorded at 100 MHz in $CDCl_3$.

Bischerbolide peroxide (**6**) was afforded as a white powder with the molecular formula $C_{40}H_{58}O_6$ from HRESIMS (*m/z* calcd 657.4124; found 657.4125, $[M + Na]^+$), appropriate for twelve degrees of unsaturation. The ^{13}C NMR spectroscopic data of **6** revealed the presence of 40 carbons (Table 2). The DEPT spectra of **6** showed the presence of eight methyls, twelve sp^3 methylenes, six sp^3 oxygenated methines, four sp^2 methines, two sp^3 and eight sp^2 nonprotoned carbons (including two ester carbonyls). NMR signals resonating at δ_C 114.3 (CH), 141.4 (C), 124.9 (C), 82.7 (CH) and 10.2 (CH_3), and δ_H 5.28 (1H, d, *J* = 10.0 Hz) and δ_H 1.72 (3H, s), and another group of signals observed at δ_C 114.4 (CH), 141.5 (C), 124.9 (C), 81.9 (CH) and 10.2 (CH_3), and δ_H 5.50 (1H, d, *J* = 10.0 Hz) and δ_H 1.73 (3H, s), revealed the presence of two slightly different 2,5-dihydrofuran rings with a peroxyl group by comparison of the similar NMR data of five-membered rings in the literature [35]. Also, two groups of signals resonating at δ_C 61.2 (C), 62.1 (CH) and δ_H 2.51 (1H, m), and δ_C 61.3 (C), 62.2 (CH) and δ_H 2.51 (1H, m) showed the presence of two trisubstituted epoxides. Four trisubstituted olefinic bonds were revealed from NMR signals appearing at δ_C 126.4 (CH), δ_C 140.2 (C) and δ_H 5.06 (1H, d, *J* = 10.0 Hz); at δ_C 125.6 (CH), δC 133.1 (C) and δ_H 4.98 (1H, dd, *J* = 9.2, 9.2 Hz); at δ_C 125.1 (CH), δ_C 141.0 (C) and δ_H 4.92 (1H, dd, *J* = 10.0 Hz); and at δ_C 125.5 (CH), δ_C 133.3 (C) and δ_H 4.95 (1H, dd, *J* = 9.2, 9.2 Hz), respectively.

As the ^{13}C NMR spectrum of **6** was constituted by twenty sets of signals with each set containing two peaks of very similar chemical shifts, **6** was thus identified as a compound formed from the connection of two quite similar diterpenoid subunits. The entire planar structure was established by examination of ^1H and ^{13}C NMR data and ^1H-^1H COSY and HMBC correlations (Figure 6). Two methines resonating at δ_C 114.3 and δ_C 114.4 were considered to be the positions at which the two cembranoidal units were connected by insertion of a peroxyl group. Based on the above analyses, the molecular skeleton of **6** was elucidated as the biscembranoid formed by the connection of two molecules of isosarcophytoxide [36] via a peroxyl group at C-16 and C-16′. The fragmentation pattern of ESIMS (Figure 7) could further prove the dimeric nature of **6** and the peroxyl linkage at C-16/C-16′. One ion peak displayed at *m/z* 339 can be explained by the cleavage of O–O bond and the following elimination of H-16 from a monocembranoidal unit in **6** to form a sodiated cembranoid lactone molecular ion A (pathway a). The other ion peaks can be interpreted by the cleavage of the single bond between C-16 and peroxyl oxygen to afford ion B (*m/z* 301), and a peroxycembranoidal radical which could further abstract an hydrogen atom and form the sodium adduct C (*m/z* 357) (pathway b). Moreover, compound **6** was found to be the first example of a biscembranoid with a molecular skeleton formed by two cembranoid units connected by a peroxyl group.

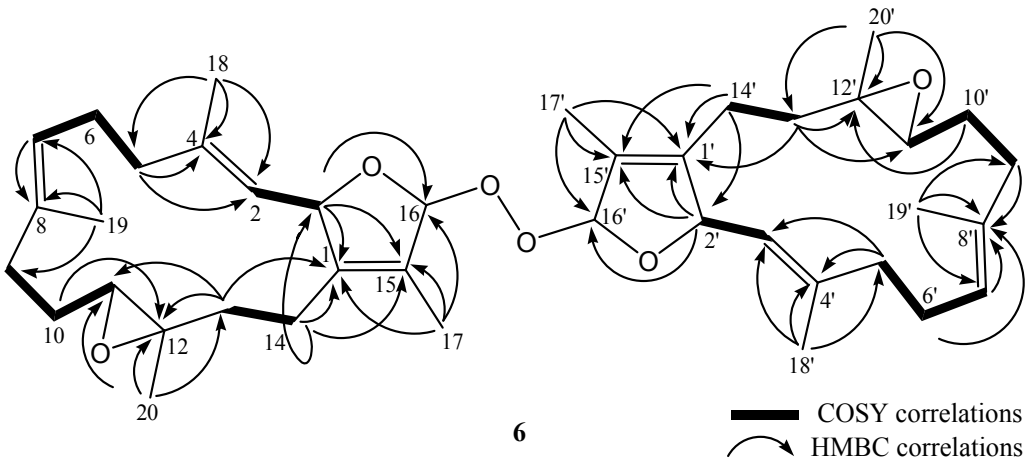

Figure 6. Selected ^1H-^1H COSY and HMBC correlations of **6**.

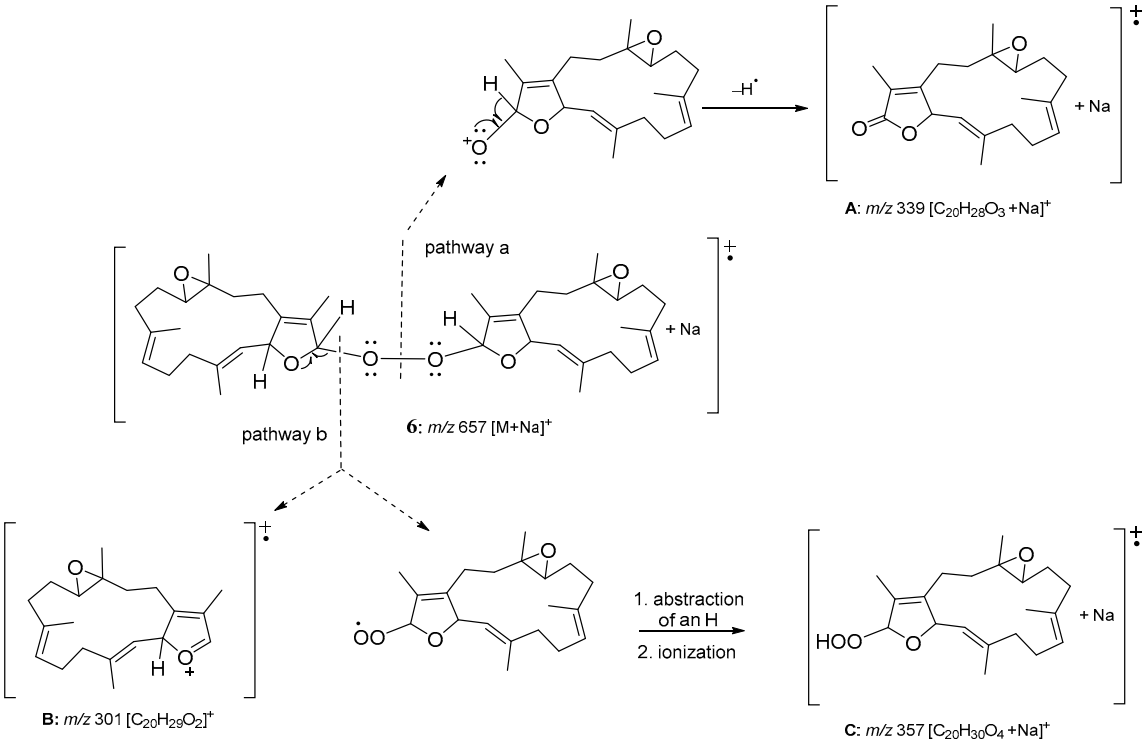

Figure 7. ESIMS fragmentation of **6**.

The relative configuration of **6** was determined from a literature survey [36,37] and NOE correlations (Figure 8). The ^{13}C NMR spectrum of **6** displayed 40 signals of two sets signals with nearly identical chemical shifts, representing the very similar stereochemical environments of the two structural units. In addition, compound **6** was found to have nearly identical chemical shifts for H-11 (11′), H_3-18 (18′), H_3-20 (20′) and C-20 (20′) to those of (2*S*,11*R*,12*R*)-isosarcophytoxide (**8**), and were in turn found to exhibit distinguishable differences to the corresponding chemical shifts of (2*R*,11*R*,12*R*)-isosarcophytoxide (**9**) (Table 3 and Figure 9). Thus, **6** possessed the cembranoidal structural unit derived from **8**, as also proven by observed NOE correlations (Figure 8). Different proton values were observed for H-2 (δ_H 5.28) and H-2′ (δ_H 5.50), indicating that H-2′ was on the same planar face as the peroxide group and was deshielded, and H-2 was on the same planar face as H-16 and was shielded. As compounds **1**−**7** were isolated from the same organism in this study, they are likely to possess the same absolute *S*,*R*,*R*-configurations at the chiral centers C-2, C-11 and C-12, respectively, as those of **1** and **3**. A previous report also showed that different absolute configurations at C-2 of the related diasteromeric dihydrofuran ring-containing cembranoids could significantly influence the sign of the specific optical rotation [36,38]. For cembranoids with 2*S* configuration a significant positive and for those with 2*R* configuration a negative optical rotation were found. The $[\alpha]_D^{25}$ of **6** was +41; thus, the absolute configuration of **6** was deduced to be 2*S*,11*R*,12*R*,16*R*, 2′*S*,11′*R*,12′*R*,16′*S*.

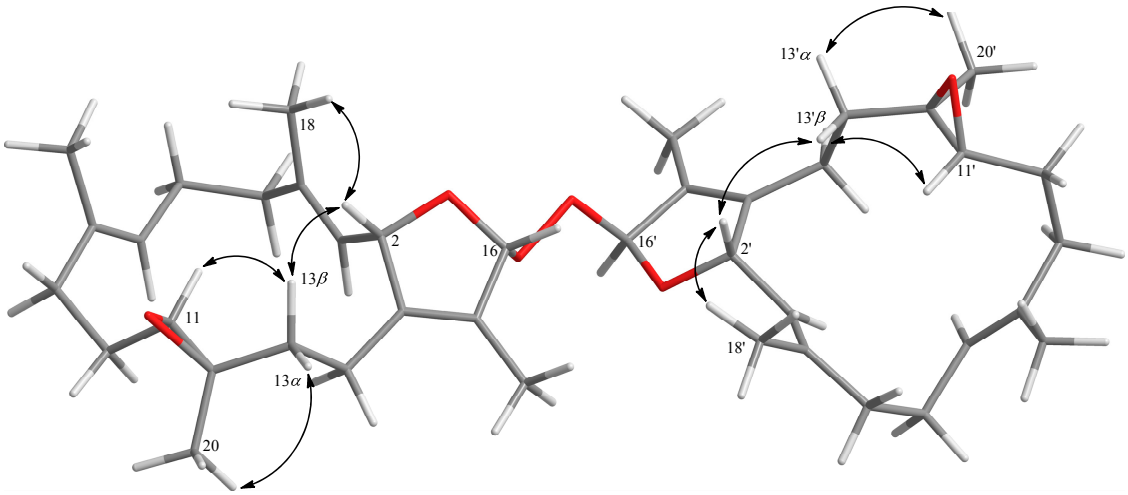

Figure 8. Selected NOESY correlations for **6**.

Table 3. Selected ^{1}H and ^{13}C NMR data comparison with **6**, (2*S*,11*R*,12*R*)-isosarcophytoxide (**8**) and (2*R*,11*R*,12*R*)-isosarcophytoxide (**9**).

Position	6	8 [a]	9 [a]
H-11	δ_H 2.51 (H-11, H-11′)	δ_H 2.50	δ_H 2.75
C-11	δ_C 62.1 (C-11) δ_C 62.2 (C-11′)	δ_C 62.3	δ_C 61.2
C-12	δ_C 61.2 (C-12) δ_C 61.3 (C-12′)	δ_C 61.4	δ_C 60.7
C-13	δ_C 37.3 (C-13) δ_C 37.4 (C-13′)	δ_C 37.4	δ_C 35.4
C-14	δ_C 22.6 (C-14) δ_C 22.7 (C-14′)	δ_C 22.5	δ_C 20.4
H_3-18	δ_H 1.58 (H_3-18) δ_H 1.59 (H_3-18′)	δ_H 1.58	δ_H 1.70
H_3-20	δ_H 1.27 (H_3-20, H_3-20′)	δ_H 1.28	δ_H 1.18
C-20	δ_C 15.7 (C-20, C-20′)	δ_C 15.7	δ_C 17.7

[a] The selected ^{1}H and ^{13}C data were cited from ref. [36,37].

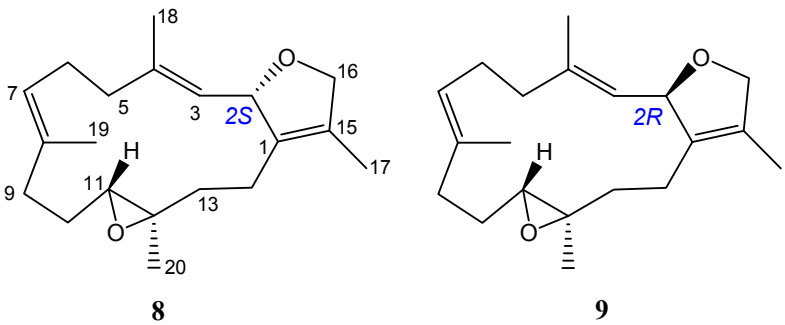

Figure 9. Structures of (2*S*,11*R*,12*R*)-isosarcophytoxide (**8**) and (2*R*,11*R*,12*R*)-isosarcophytoxide (**9**) [36].

The plausible biosynthesis of **6** might arise from the proton abstraction at C-16 of **8** by hydrogen peroxide radical HOO• to form a radical intermediate **10**, which could react with O_2 from one plane side of radical center C-16 to afford cembranoidal peroxide radical **11**. Further reaction of **11** with **10** from another side could lead to the formation of **6** (Scheme 1). However, the possibility that **6** might be generated by autooxidation of **8** could not be neglected.

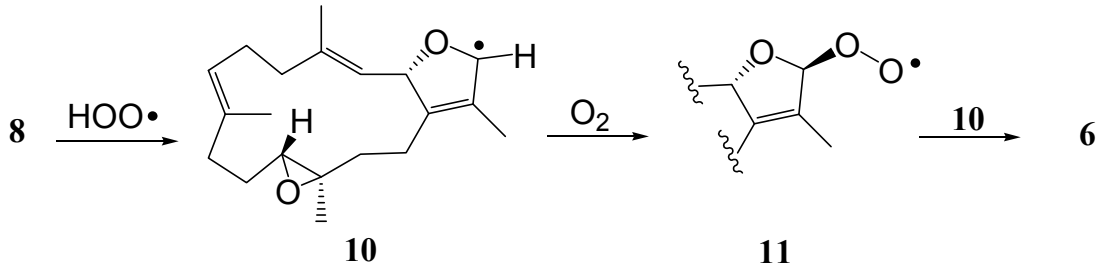

Scheme 1. Proposed biosynthetic pathway for **6**.

It is known that the proteolytic enzymes and toxic reactive oxygen species produced by stimulated neutrophils might play a critical role in the pathogenesis of many inflammatory diseases [39,40]. By measuring the capability to inhibit *N*-formyl-methionyl-leucyl-phenylalanine/cytochalasin B (fMLF/CB)-induced superoxide anion generation and elastase release in human neutrophils, the in vitro anti-inflammatory effects for metabolites **1**–**7** were evaluated [41,42]. According to the results (shown in Table 4), compound **6** had a significant inhibitory effect (64.6 ± 0.8%), with an IC_{50} value of 26.2 ± 1.0 μM, on the generation of superoxide anions, and compounds **1** and **3** had moderate inhibitory effects (32.1 ± 4.3% and 44.5 ± 4.6%, respectively) at 30 μM. Compounds **1**, **3** and **6** revealed moderate inhibitory effects (37.6 ± 5.0%, 35.6 ± 6.2% and 42.4 ± 5.1%, respectively) on elastase release at the same concentration. These results, obtained after stimualting the neutrophils with fMLF/CB, may suggest that **1**, **3** and **6** have potential merits against inflammatory disorders.

Table 4. Inhibitory effects of compounds **1**–**7** on superoxide anion generation and elastase release in fMLF/CB-induced human neutrophils.

Compounds	Superoxide Anion		Elastase Release
	IC_{50} (μM) [a]	Inh [b] %	Inh [b] %
1	>30	32.1 ± 4.3 **	37.6 ± 5.0 **
2	>30	4.0 ± 6.7	23.5 ± 6.6 *
3	>30	44.5 ± 4.6 ***	35.6 ± 6.2 **
4	>30	6.4 ± 4.2	27.6 ± 6.4 **
5	>30	2.6 ± 6.2	30.5 ± 4.6 **
6	26.2 ± 1.0	64.6 ± 0.8 ***	42.4 ± 5.1 **
7	>30	3.5 ± 5.3	20.7 ± 4.1 **
Idelalisib	0.07 ± 0.01	102.8 ± 2.2 ***	99.6 ± 4.2

[a] Concentration necessary for 50% inhibition (IC_{50}). [b] Percentage of inhibition (Inh %) at 30 μM. Data are presented as mean ± S.E.M. (n = 3–4); * $p < 0.05$, ** $p < 0.01$, *** $p < 0.001$ compared with the control value.

In summary, examination of the chemical constituents of the soft coral *Sarcophyton cherbonnieri* led to the discovery of six new compounds **1**–**6**, along with one known compound **7**. Although a number of natural compounds possessing a peroxyl group, such as artemisinin [43], neovibsanin C [44], cardamom peroxide [45], plakortin [46] and chondrillin [47], have been discovered, compound **6** was discovered to be the first compound with a molecular skeleton consisting of two cembranoidal units connected by a peroxide group. Similar to the results of previous studies indicating that natural peroxides could possess promising biological activity [48], compound **6** was found to possess anti-inflammatory activity by exhibiting stronger ability on inhibition on the generation of superoxide anions and release of elastase in fMLF/CB-induced human neutrophils.

3. Materials and Methods

3.1. General Procedures

The values of optical rotation of the metabolites were determined with a JASCO P-1020 polarimeter (JASCO Corporation, Tokyo, Japan). Infrared absorptions were recorded using a JASCO FT/IR-4100 infrared spectrophotometer (JASCO Corporation, Tokyo, Japan). ^{1}H and ^{13}C NMR spectra were obtained on a Varian 400MR FT-NMR (or Varian Unity INOVA500 FT-NMR) instrument (Varian Inc., Palo Alto, CA, USA) at 400 MHz (or 500 MHz) and 100 MHz (or 125 MHz), respectively, in $CDCl_3$ or C_6D_6. The data of LRESIMS and HRESIMS were measured using a Bruker APEX II (Bruker, Bremen, Germany) mass spectrometer. Silica gel (230–400 mesh) was used as adsorbent for column chromatography. TLC analyses were performed using precoated silica gel plates (Kieselgel 60 F-254, 0.2 mm) (Merck, Darmstadt, Germany). Further purification of impure fractions or compounds were performed by high-performance liquid chromatography on a Hitachi L-7100 HPLC instrument (Hitachi Ltd., Tokyo, Japan) with a Merck Hibar Si-60 column (250 mm × 21 mm, 7 μm; Merck, Darmstadt, Germany) and on a Hitachi L-2455 HPLC apparatus (Hitachi, Tokyo, Japan) with a Supelco C18 column (250 mm × 21.2 mm, 5 μm; Supelco, Bellefonte, PA, USA).

3.2. Animal Material

The soft coral *S. cherbonnieri* was collected by hand using scuba diving from Jihui Fish Port, Taiwan, in March 2013, at a depth of 10–15 m. Organisms of the marine animal were stored in a freezer until extraction.

3.3. Extraction and Isolation

The frozen marine organisms, *S. cherbonnieri* (1.2 kg, wet wt), were freeze-dried (yield: 207 g), minced to small pieces and then extracted thoroughly with EtOAc (1 L × 5). The combined EtOAc extract (10.2 g) was concentrated under reduced pressure to yield a residue, which was chromatographed over a silica gel column by eluting with acetone in *n*-hexane (0–100%, stepwise), and then with MeOH in acetone (0–100%, stepwise) to yield 19 fractions. Fraction 9, eluting with *n*-hexane–acetone (6:1), was repeatedly purified by column chromatography over silica gel to yield a solid which was immersed in cold MeOH (0 °C) to afford a white powder **6** (24.3 mg). Fraction 10, eluting with *n*-hexane–acetone (4:1), was further purified over silica gel using *n*-hexane–acetone (6:1) to afford seven subfractions (A1–A7) and afford **7** (320.4 mg). Subfraction A2 was further separated by reverse-phase HPLC using acetonitrile–H_2O (1:1.3) to afford **1** (11.0 mg). Subfraction A3 was purified by reverse-phase HPLC using acetonitrile–H_2O (1:1.1) to afford **2** (13.3 mg) and **5** (10.1 mg). Fraction 13, eluting with *n*-hexane–acetone (1:1), eluting with acetone by sephadex LH-20 to afford five subfractions (B1–B5). Subfraction B3 was purified by reverse-phase HPLC using acetonitrile–H_2O (1:1.4) to afford **3** (10.6 mg) and **4** (9.4 mg).

3.3.1. Cherbonnolide A (**1**)

Colorless oil; $[\alpha]_D^{25}$ +43 (*c* 1.00, $CHCl_3$); IR (neat) ν_{max} 3444, 1746, and 1003 cm^{-1}; ^{13}C and ^{1}H NMR data see Table 1; HRMS (ESI-TOF) *m/z*: [M + Na]$^+$ Calcd for $C_{20}H_{28}O_4Na$ 355.1880; Found 355.1879.

3.3.2. Cherbonnolide B (**2**)

Colorless oil; $[\alpha]_D^{25}$ +59 (*c* 1.00, $CHCl_3$); IR (neat) ν_{max} 3363, 1741, 1678, and 1093 cm^{-1}; ^{13}C and ^{1}H NMR data see Table 1; HRMS (ESI-TOF) *m/z*: [M + Na]$^+$ Calcd for $C_{20}H_{28}O_5Na$ 371.1829; Found 371.1830.

3.3.3. Cherbonnolide C (**3**)

Colorless oil; $[\alpha]_D^{25}$ +26 (*c* 1.00, $CHCl_3$); IR (neat) ν_{max} 3445, 1749, 1678, and 1094 cm^{-1}; ^{13}C and ^{1}H NMR data see Table 1; HRMS (ESI-TOF) *m/z*: $[M + Na]^+$ Calcd for $C_{20}H_{28}O_4Na$ 355.1880; Found 355.1882.

3.3.4. Cherbonnolide D (**4**)

White powder; $[\alpha]_D^{25}$ +3 (*c* 1.00, $CHCl_3$); IR (neat) ν_{max} 3445, 1748, and 1096 cm^{-1}; ^{13}C and ^{1}H NMR data see Table 1; HRMS (ESI-TOF) *m/z*: $[M + Na]^+$ Calcd for $C_{20}H_{28}O_4Na$ 355.1880; Found 355.1883.

3.3.5. Cherbonnolide E (**5**)

Colorless oil; $[\alpha]_D^{25}$ +8 (*c* 1.00, $CHCl_3$); IR (neat) ν_{max} 3389, 1748, 1678 and 1096 cm^{-1}; ^{13}C and ^{1}H NMR data see Table 2; HRMS (ESI-TOF) *m/z*: $[M + Na]^+$ Calcd for $C_{20}H_{28}O_5Na$ 371.1829; Found 371.1830.

3.3.6. Bischerbolide Peroxide (**6**)

White powder; $[\alpha]_D^{25}$ +41 (*c* 1.00, $CHCl_3$); IR (neat) ν_{max} 3420, 1733, 1232, 1166 and 1040 cm^{-1}; ^{13}C and ^{1}H NMR data see Table 2; HRMS (ESI-TOF) *m/z*: $[M + Na]^+$ Calcd for $C_{40}H_{58}O_6Na$ 657.4125; Found 657.4124.

3.3.7. Reduction of Cherbonolides B and E (**2** and **5**)

In diethyl ether (5.0 mL), compound **2** (3.2 mg) was added followed by addition of excess amount of triphenylphosphine (2.9 mg) and the mixture was stirred at room temperature for 4 h. The solvent of the solution was evaporated under reduced pressure to afford a residue, which was purified by silica gel column chromatography using *n*-hexane–acetone (3:1) as an eluent to yield **1** (2.9 mg, 95%). Similarly, **5** (2.1 mg) was converted to **4** (1.7 mg) in 85% yield.

3.3.8. Preparation of (*S*)- and (*R*)- MTPA Esters of **1** and **3**

Compound **1** (1.3 mg) was dissolved in pyridine 100 μL and added (*R*)-(−)-*α*-methoxy-*α*-(trifluoromethyl) phenylacetyl chloride (MTPA chloride) 10 μL. The mixture was permitted to stand at room temperature overnight and the reaction was found to complete by monitoring with normal-phase TLC plate. The solution was dried completely under the vacuum of an oil pump and the residue was purified by a short silica gel column using acetone to *n*-hexane (1:3) to yield the (*S*)-MTPA ester **1a** (0.9 mg, 62.9%). The same procedure was applied to obtain the (*R*)-MTPA ester **1b** (1.0 mg, 69.9%) from the reaction of (*S*)-(+)-*α*-methoxy-*α*-(trifluoromethyl) phenylacetyl chloride with **1** in pyridine. Selective ^{1}H NMR ($CDCl_3$, 400 MHz) data of **1a**: δ_H 4.925 (1H, d, *J* = 10.0 Hz, H-3), 1.769 (3H, s, H_3-18), 2.821 (1H, dd, *J* = 12.8, 4.8 Hz, H-5a), 2.376 (1H, m, H-5b), 5.107 (1H, d, *J* = 9.6 Hz, H-7), 1.880 (3H, s, H_3-19), 2.460 (1H, m, H-9a), 1.989 (1H, m, H-9b); selective ^{1}H NMR ($CDCl_3$, 400 MHz) data of **1b**: δ_H 4.905 (1H, d, *J* = 10.0 Hz, H-3), 1.763 (3H, s, H_3-18), 2.739 (1H, dd, *J* = 12.8, 5.6 Hz, H-5a), 2.267 (1H, m, H-5b), 5.217 (1H, d, *J* = 9.6 Hz, H-7), 1.905 (3H, s, H_3-19), 2.476 (1H, m, H-9a), 1.998 (1H, m, H-9b).

Preparation of (*S*)- and (*R*)- MTPA esters of **3** used the same reaction and purification procedures as the reduction of **1**, the solution of **3** (1.1 mg) was converted to the (*S*)-MTPA ester **3a** (0.8 mg) in 74% yield and (*R*)-MTPA ester **3b** (0.9 mg) in 80% yield, respectively. Selective ^{1}HNMR (C_6D_6, 400 MHz) data of **3a**: δ_H 1.243 (3H, s, H_3-18), 2.311 (1H, dd, *J* = 11.2, 2.4 Hz, H-5a), 1.930 (1H, dd, *J* = 11.2, 11.2 Hz, H-5b), 5.065 (1H, d, *J* = 9.2 Hz, H-7), 1.416 (3H, s, H_3-19); selective ^{1}H NMR (C_6D_6, 400 MHz) data of **3b**: δ_H 1.244 (3H, s, H_3-18), 2.363 (1H, dd, *J* = 12.0, 3.2 Hz, H-5a), 1.982 (1H, dd, *J* = 12.0, 11.6 Hz, H-5b), 4.9515 (1H, d, *J* = 10.0 Hz, H-7), 1.360 (3H, s, H_3-19).

3.4. In Vitro Anti-Inflammatory Testing

3.4.1. Human Neutrophils

Blood was obtained from elbow vein of healthy adult volunteers (years 20–30). Neutrophils were enriched by dextran sedimentation, Ficoll-Hypaque centrifugation, and hypotonic lysis. Neutrophils were incubated in an ice-cold Ca^{2+}-free HBSS buffer (pH 7.4) [42].

3.4.2. Superoxide Anion Generation

Neutrophils (6×10^5 cells mL^{-1}) incubated in HBSS with ferricytochrome *c* (0.5 mg mL^{-1}) and Ca^{2+} (1 mM) at 37 °C were treated with DMSO (as control) or compound for 5 min. Neutrophils were primed by cytochalasin B (CB, 1 μg mL^{-1}) for 3 min before activating fMLF (100 nM) for 10 min (fMLF/CB) [40,49].

3.4.3. Elastase Release

Neutrophils (6×10^5 cells mL^{-1}) incubated in HBSS with MeO-Suc-Ala-Ala-Pro-Val-*p*-nitroanilide (100 μM) and Ca^{2+} (1 mM) at 37 °C were treated with DMSO or compound for 5 min. Neutrophils were activated with fMLF (100 nM)/CB (0.5 μg mL^{-1}) for 10 min [40].

3.4.4. Statistical Analysis

Data are displayed as the mean ± SEM and comparisons were performed by Student's *t*-test. A probability value of 0.05 or less was considered to be significant. The software Sigma Plot (version 8.0, Systat Software, San Jose, CA, USA) was used for the statistical analysis.

4. Conclusions

Six new cembranoids, cherbonolides A−E (**1**–**5**) and a cembrane dimer (bischerbolide peroxide, **6**), along with isosarcophine (**7**) were isolated from the Formosan soft coral *Sarcophyton cherbonnieri*. Bischerbolide peroxide (**6**) was discovered as the first example of cembranoid dimers possessing a peroxide group as a linking group. Compounds **1**, **3** and **6** showed an anti-inflammatory activity through their inhibitory effects on the generation of superoxide anion in fMLP/CB-induced human neutrophils. Moreover, peroxide **6** was also shown to exhibit stronger activity in inhibiting the elastase release which supported its anti-inflammatory activity.

Supplementary Materials: HRESIMS, ^{1}H, ^{13}C, DEPT, HMQC, COSY, HMBC and NOESY spectra of new compounds **1**–**6**, and ^{1}H NMR spectra of (+)-sarcophytoxide and sarcophytonin after different treatments are available online at http://www.mdpi.com/1660-3397/16/8/276/s1. Figure S1: HRESIMS spectrum of **1**, Figure S2: ^{1}H NMR spectrum of **1** in $CDCl_3$, Figure S3: ^{13}C NMR spectrum of **1** in $CDCl_3$, Figure S4: HSQC spectrum of **1** in $CDCl_3$, Figure S5: ^{1}H-^{1}HCOSY spectrum of **1** in $CDCl_3$, Figure S6: HMBC spectrum of **1** in $CDCl_3$, Figure S7: NOESY spectrum of **1** in $CDCl_3$, Figure S8: HRESIMS spectrum of **2**, Figure S9: ^{1}H NMR spectrum of **2** in $CDCl_3$, Figure S10: ^{13}C NMR spectrum of **2** in $CDCl_3$, Figure S11: HSQC spectrum of **2** in $CDCl_3$, Figure S12: ^{1}H-^{1}HCOSY spectrum of **2** in $CDCl_3$, Figure S13: HMBC spectrum of **2** in $CDCl_3$, Figure S14: NOESY spectrum of **2** in $CDCl_3$, Figure S15: HRESIMS spectrum of **3**, Figure S16: ^{1}H NMR spectrum of **3** in C_6D_6, Figure S17: ^{13}C NMR spectrum of **1** in C_6D_6, Figure S18: HSQC spectrum of **1** in C_6D_6, Figure S19: ^{1}H-^{1}HCOSY spectrum of **3** in C_6D_6, Figure S20: HMBC spectrum of **3** in C_6D_6, Figure S21: NOESY spectrum of **3** in C_6D_6, Figure S22: HRESIMS spectrum of **4**, Figure S23: ^{1}H NMR spectrum of **4** in C_6D_6, Figure S24: ^{13}C NMR spectrum of **4** in C_6D_6, Figure S25: HSQC spectrum of **4** in C_6D_6, Figure S26: ^{1}H-^{1}HCOSY spectrum of **4** in C_6D_6, Figure S27: HMBC spectrum of **4** in C_6D_6, Figure S28: NOESY spectrum of **4** in C_6D_6, Figure S29: HRESIMS spectrum of **5**, Figure S30: ^{1}H NMR spectrum of **5** in C_6D_6, Figure S31: ^{13}C NMR spectrum of **5** in C_6D_6, Figure S32: HSQC spectrum of **5** in C_6D_6, Figure S33: ^{1}H-^{1}HCOSY spectrum of **5** in C_6D_6, Figure S34: HMBC spectrum of **5** in C_6D_6, Figure S35: NOESY spectrum of **5** in C_6D_6, Figure S36: HRESIMS spectrum of **6**, Figure S37: ESIMS spectrum of **6**, S38: ^{1}H NMR spectrum of **6** in $CDCl_3$, Figure S39: ^{13}C NMR spectrum of **6** in $CDCl_3$, Figure S40: HSQC spectrum of **6** in $CDCl_3$, Figure S41: ^{1}H-^{1}HCOSY spectrum of **6** in $CDCl_3$, Figure S42: HMBC spectrum of **6** in $CDCl_3$, Figure S43: NOESY spectrum of **6** in $CDCl_3$, Figure S44: ^{1}H NMR spectrum of (+)-sarcophytoxide in $CDCl_3$ before treatment with acetone and silica gel under air, Figure S45. ^{1}H NMR spectrum of (+)-sarcophytoxide

in $CDCl_3$ after treatment with acetone and silica gel under air, Figure S46. ^{1}H NMR spectrum of sarcophytonin A in $CDCl_3$ before treatment with acetone and silica gel under air, Figure S47. ^{1}H NMR spectrum of sarcophytonin A in $CDCl_3$ after treatment with acetone and silica gel under air.

Author Contributions: J.-H.S. conceived and guided the whole experiment. C.-C.P. isolated the compounds, and performed spectroscopic data measurement and analysis, and structure interpretation. C.-Y.H. and A.F.A. performed spectroscopic data analysis, confirmation of structures and preparation of the manuscript. T.-L.H. performed the anti-inflammatory assay. C.-F.D. contributed to species identification of the soft coral.

Funding: This research was funded by Ministry of Science and Technology of Taiwan (MOST102-2113-M-110-001-MY2, 104-2113-M-110-006, and 104-2811-M-110-026) and International Scientific Partnership Program (ISPP) at King Saud University, Saudi Arabia (ISPP-116).

Acknowledgments: Financial supported was mainly provided by the Ministry of Science and Technology (MOST102-2113-M-110-001-MY2, 104-2113-M-110-006, and 104-2811-M-110-026) to J.-H.S. The authors extend their appreciation to the International Scientific Partnership Program ISPP at King Saud University for funding this research work through ISPP-116.

Conflicts of Interest: The authors declare no conflict of interest.

References

1. Farag, M.A.; Fekry, M.I.; Al-Hammady, M.A.; Khalil, M.N.; El-Seedi, H.R.; Meyer, A.; Porzel, A.; Westphal, H.; Wessjohann, L.A. Cytotoxic effects of *Sarcophyton* sp. soft corals-Is there a correlation to their NMR fingerprints? *Mar. Drugs* **2017**, *15*, 211. [CrossRef] [PubMed]
2. Chao, C.H.; Li, W.L.; Huang, C.Y.; Ahmed, A.F.; Dai, C.F.; Wu, Y.C.; Lu, M.C.; Liaw, C.C.; Sheu, J.H. Isoprenoids from the soft coral *Sarcophyton glaucum*. *Mar. Drugs* **2017**, *15*, 202. [CrossRef] [PubMed]
3. Hegazy, M.E.F.; Elshamy, A.I.; Mohamed, T.A.; Hamed, A.R.; Ibrahim, M.A.A.; Ohta, S.; Pare, P.W. Cembrene diterpenoids with ether linkages from *Sarcophyton ehrenbergi*: An anti-proliferation and molecular-docking assessment. *Mar. Drugs* **2017**, *15*, 192. [CrossRef] [PubMed]
4. Elkhateeb, A.; El-Beih, A.A.; Gamal-Eldeen, A.M.; Alhammady, M.A.; Ohta, S.; Pare, P.W.; Hegazy, M.E.F. New terpenes from the Egyptian soft coral *Sarcophyton ehrenbergi*. *Mar. Drugs* **2014**, *12*, 1977–1986. [CrossRef] [PubMed]
5. Eltahawy, N.A.; Ibrahim, A.K.; Radwan, M.M.; ElSohly, M.A.; Hassanean, H.A.; Hassanean, H.A.; Ahmed, S.A. Cytotoxic cembranoids from the Red Sea soft coral, *Sarcophyton auritum*. *Tetrahedron Lett.* **2014**, *55*, 3984–3988. [CrossRef]
6. Lin, W.Y.; Lu, Y.; Su, J.H.; Wen, Z.H.; Dai, C.F.; Kuo, Y.H.; Sheu, J.H. Bioactive cembranoids from the dongsha atoll soft coral *Sarcophyton crassocaule*. *Mar. Drugs* **2011**, *9*, 994–1006. [CrossRef] [PubMed]
7. Lin, W.Y.; Su, J.H.; Lu, Y.; Wen, Z.H.; Dai, C.F.; Kuo, Y.H.; Sheu, J.H. Cytotoxic and anti-inflammatory cembranoids from the Dongsha Atoll soft coral *Sarcophyton crassocaule*. *Bioorg. Med. Chem.* **2010**, *18*, 1936–1941. [CrossRef] [PubMed]
8. Iwagawa, T.; Hashimoto, K.; Yokogawa, Y.; Okamura, H.; Nakatani, M.; Doe, M.; Morimoto, Y.; Takemura, K. Cytotoxic biscembranes from the soft coral *Sarcophyton glaucum*. *J. Nat. Prod.* **2009**, *72*, 946–949. [CrossRef] [PubMed]
9. Huang, C.Y.; Tseng, Y.J.; Chokkalingam, U.; Hwang, T.L.; Hsu, C.H.; Dai, C.F.; Sung, P.J.; Sheu, J.H. Bioactive isoprenoid-derived natural products from a Dongsha Atoll soft coral *Sinularia erecta*. *J. Nat. Prod.* **2016**, *79*, 1339–1346. [CrossRef] [PubMed]
10. Tseng, Y.J.; Yang, Y.C.; Wang, S.K.; Duh, C.Y. Numerosol A-D, new cembranoid diterpenes from the soft coral *Sinularia numerosa*. *Mar. Drugs* **2014**, *12*, 3371–3380. [CrossRef] [PubMed]
11. Lillsunde, K.E.; Festa, C.; Adel, H.; De Marino, S.; Lombardi, V.; Tilvi, S.; Nawrot, D.A.; Zampella, A.; D'Souza, L.; D'Auria, M.V.; et al. Bioactive cembrane derivatives from the Indian Ocean soft coral, *Sinularia kavarattiensis*. *Mar. Drugs* **2014**, *12*, 4045–4068. [CrossRef] [PubMed]
12. Li, G.; Zhang, Y.; Deng, Z.; van Ofwegen, L.; Proksch, P.; Lin, W. Cytotoxic cembranoid diterpenes from a soft coral *Sinularia gibberosa*. *J. Nat. Prod.* **2005**, *68*, 649–652. [CrossRef] [PubMed]
13. Cheng, S.Y.; Wen, Z.H.; Wang, S.K.; Chiou, S.F.; Hsu, C.H.; Dai, C.F.; Chiang, M.Y.; Duh, C.Y. Unprecedented hemiketal cembranolides with anti-inflammatory activity from the soft coral *Lobophytum durum*. *J. Nat. Prod.* **2009**, *72*, 152–155. [CrossRef] [PubMed]

14. Chao, C.H.; Wen, Z.H.; Wu, Y.C.; Yeh, H.C.; Sheu, J.H. Cytotoxic and anti-inflammatory cembranoids from the soft coral *Lobophytum crassum*. *J. Nat. Prod.* **2008**, *71*, 1819–1824. [CrossRef] [PubMed]
15. Lai, K.H.; You, W.J.; Lin, C.C.; El-Shazly, M.; Liao, Z.J.; Su, J.H. Anti-Inflammatory cembranoids from the soft coral *Lobophytum crassum*. *Mar. Drugs* **2017**, *15*, 327. [CrossRef] [PubMed]
16. Lin, K.H.; Tseng, Y.J.; Chen, B.W.; Hwang, T.L.; Chen, H.Y.; Dai, C.F.; Sheu, J.H. Tortuosenes A and B, new diterpenoid metabolites from the Formosan soft coral *Sarcophyton tortuosum*. *Org. Lett.* **2014**, *16*, 1314–1317. [CrossRef] [PubMed]
17. Chao, C.H.; Wu, C.Y.; Huang, C.Y.; Wang, H.C.; Dai, C.F.; Wu, Y.C.; Sheu, J.H. Cubitanoids and cembranoids from the soft coral *Sinularia nanolobata*. *Mar. Drugs* **2016**, *14*, 150. [CrossRef] [PubMed]
18. Chen, B.W.; Chao, C.H.; Su, J.H.; Huang, C.Y.; Dai, C.F.; Wen, Z.H.; Sheu, J.H. A novel symmetric sulfur-containing biscembranoid from the formosan soft coral *Sinularia flexibilis*. *Tetrahedron Lett* **2010**, *51*, 764–766. [CrossRef]
19. Huang, C.Y.; Sung, P.J.; Uvarani, C.; Su, J.H.; Lu, M.C.; Hwang, T.L.; Dai, C.F.; Wu, S.L.; Sheu, J.H. Glaucumolides A and B, biscembranoids with new structural type from a cultured soft coral *Sarcophyton glaucum*. *Sci. Rep.* **2015**, *5*, 15624. [CrossRef] [PubMed]
20. Jia, R.; Kurtan, T.; Mandi, A.; Yan, X.H.; Zhang, W.; Guo, Y.W. Biscembranoids formed from an alpha, beta-unsaturated gamma-lactone ring as a dienophile: Structure revision and establishment of their absolute configurations using theoretical calculations of electronic circular dichroism spectra. *J. Org. Chem.* **2013**, *78*, 3113–3119. [CrossRef] [PubMed]
21. Kusumi, T.; Igari, M.; Ishitsuka, M.O.; Ichikawa, A.; Itezono, Y.; Nakayama, N.; Kakisawa, H. A Novel chlorinated biscembranoid from the marine soft coral *Sarcophyton glaucum*. *J. Org. Chem.* **1990**, *55*, 6286–6289. [CrossRef]
22. Tseng, Y.J.; Ahmed, A.F.; Dai, C.F.; Chiang, M.Y.; Sheu, J.H. Sinulochmodins A-C, three novel terpenoids from the soft coral *Sinularia lochmodes*. *Org. Lett.* **2005**, *7*, 3813–3816. [CrossRef] [PubMed]
23. Li, Y.; Pattenden, G. Biomimetic syntheses of ineleganolide and sinulochmodin C from 5-episinuleptolide via sequences of transannular Michael reactions. *Tetrahedron* **2011**, *67*, 10045–10052. [CrossRef]
24. Kusumi, T.; Yamada, K.; Ishitsuka, M.O.; Fujita, Y.; Kakisawa, H. New cembranoids from the Okinawan soft coral *Sinularia mayi*. *Chem. Lett.* **1990**, *19*, 1315–1318. [CrossRef]
25. Uchio, Y.; Eguchi, S.; Kuramoto, J.; Nakayama, M.; Hase, T. Denticulatolide, an ichthyotoxic peroxide-containing cembranolide from the soft coral *Lobophytum denticulatum*. *Tetrahedron Lett.* **1985**, *26*, 4487–4490. [CrossRef]
26. Hegazy, M.E.; Gamal Eldeen, A.M.; Shahat, A.A.; Abdel-Latif, F.F.; Mohamed, T.A.; Whittlesey, B.R.; Pare, P.W. Bioactive hydroperoxyl cembranoids from the Red Sea soft coral *Sarcophyton glaucum*. *Mar. Drugs* **2012**, *10*, 209–222. [CrossRef] [PubMed]
27. Casteel, D.A. Peroxy natural products. *Nat. Prod. Rep.* **1992**, *9*, 289–312. [CrossRef] [PubMed]
28. Liang, L.F.; Chen, W.T.; Li, X.W.; Wang, H.Y.; Guo, Y.W. New bicyclic cembranoids from the South China Sea soft coral *Sarcophyton trocheliophorum*. *Sci. Rep.* **2017**, *7*, 46584. [CrossRef] [PubMed]
29. Zhao, M.; Yin, J.; Jiang, W.; Ma, M.; Lei, X.; Xiang, Z.; Dong, J.; Huang, K.; Yan, P. Cytotoxic and antibacterial cembranoids from a South China Sea soft coral, *Lobophytum* sp. *Mar. Drugs* **2013**, *11*, 1162–1172. [CrossRef] [PubMed]
30. Kalinowski, H.O.; Berger, S.; Braun, S. *Carbon-13 NMR Spectroscopy*; John Wiley & Sons: Chichester, UK, 1988.
31. Dale, J.A.; Mosher, H.S. Nuclear magnetic resonance enantiomer regents. Configurational correlations via nuclear magnetic resonance chemical shifts of diastereomeric mandelate, *O*-methylmandelate, and alpha-methoxy-alpha-trifluoromethylphenylacetate (MTPA) esters. *J. Am. Chem. Soc.* **1973**, *95*, 512–519. [CrossRef]
32. Ohtani, I.; Kusumi, T.; Kashman, Y.; Kakisawa, H. High-Field FT NMR application of Mosher's method. The absolute configurations of marine terpenoids. *J. Am. Chem. Soc.* **1991**, *113*, 4092–4096. [CrossRef]
33. Duh, C.Y.; Chia, M.C.; Wang, S.K.; Chen, H.J.; El-Gamal, A.A.; Dai, C.F. Cytotoxic dolabellane diterpenes from the Formosan soft coral *Clavularia inflata*. *J. Nat. Prod.* **2001**, *64*, 1028–1031. [CrossRef] [PubMed]
34. Corminboeuf, O.; Overman, L.E.; Pennington, L.D. Total synthesis of the reputed structure of alcyonin and reassignment of its structure. *Org. Lett.* **2003**, *5*, 1543–1546. [CrossRef] [PubMed]

35. Chen, S.P.; Chen, B.W.; Dai, C.F.; Sung, P.J.; Wu, Y.C.; Sheu, J.H. Sarcophyton F and G new dihydrofuranocembranoids from a Donsha atoll soft coral *Sarcophyton* sp. *Bull. Chem. Soc. Jpn.* **2012**, *85*, 920–922. [CrossRef]
36. Bowden, B.F.; Coll, J.C.; Heaton, A.; Konig, G.; Bruck, M.A.; Cramer, R.E.; Klein, D.M.; Scheuer, P.J. The structure of four isometric dihydrofuran-containing cembranoid diterpenes from several species of soft corals. *J. Nat. Prod.* **1987**, *50*, 650–659. [CrossRef]
37. Bowden, B.F.; Coll, J.C. Studies of Australian soft corals. XLV. Epoxidation reaction of cembranoid diterpenes: Stereochemical outcomes. *Heterocycles* **1989**, *28*, 669–672. [CrossRef]
38. Kobayashi, M.; Hirase, T. Marine terpenes and terpenoids. XI. Structures of new dihydrofuranocembranoids isolated from a *Sarcophyton* sp. soft coral of Okinawa. *Chem. Pharm. Bull.* **1990**, *38*, 2442–2445. [CrossRef]
39. Mantovani, A.; Cassatella, M.A.; Costantini, C.; Jaillon, S. Neutrophils in the activation and regulation of innate and adaptive immunity. *Nat. Rev. Immunol.* **2011**, *11*, 519–531. [CrossRef] [PubMed]
40. Yang, S.C.; Chung, P.J.; Ho, C.M.; Kuo, C.Y.; Hung, M.F.; Huang, Y.T.; Chang, W.Y.; Chang, Y.W.; Chan, K.H.; Hwang, T.L. Propofol inhibits superoxide production, elastase release, and chemotaxis in formyl peptide-activated human neutrophils by blocking formyl peptide receptor 1. *J. Immunol.* **2013**, *190*, 6511–6519. [CrossRef] [PubMed]
41. Hwang, T.L.; Li, G.L.; Lan, Y.H.; Chia, Y.C.; Hsieh, P.W.; Wu, Y.H.; Wu, Y.C. Potent inhibition of superoxide anion production in activated human neutrophils by isopedicin, a bioactive component of the Chinese medicinal herb Fissistigma oldhamii. *Free. Radic. Biol. Med.* **2009**, *46*, 520–528. [CrossRef] [PubMed]
42. Hwang, T.L.; Su, Y.C.; Chang, H.L.; Leu, Y.L.; Chung, P.J.; Kuo, L.M.; Chang, Y.J. Suppression of superoxide anion and elastase release by C18 unsaturated fatty acids in human neutrophils. *J. Lipid Res.* **2009**, *50*, 1395–1408. [CrossRef] [PubMed]
43. Tu, Y. The discovery of artemisinin (qinghaosu) and gifts from Chinese medicine. *Nat. Med.* **2011**, *17*, 1217–1220. [CrossRef] [PubMed]
44. Kubo, M.; Minami, H.; Hayashi, E.; Kodama, M.; Kawazu, K.; Fukuyama, Y. Neovibsanin C, a macrocyclic peroxide-containing neovibsane-type diterpene from *Viburnum awabuki*. *Tetrahedron Lett.* **1999**, *40*, 6261–6265. [CrossRef]
45. Kamchonwongpaisan, S.; Nilanonta, C.; Tarnchompoo, B.; Thebtaranonth, C.; Thebtaranonth, Y.; Yuthavong, Y.; Kongsaeree, P.; Clardy, J. An antimalarial peroxide from *Amomum krervanh* Pierre. *Tetrahedron Lett.* **1995**, *36*, 1821–1824. [CrossRef]
46. Higgs, M.D.; Faulkner, D.J. Plakortin, an antibiotic from *Plakortis halichondrioides*. *J. Org. Chem.* **1978**, *34*, 3454–3457. [CrossRef]
47. Wells, R.J. A novel peroxyketal from a sponge. *Tetrahedron Lett.* **1976**, *17*, 2637–2638. [CrossRef]
48. Bu, M.; Yang, B.B.; Hu, L. Natural endoperoxides as drug lead compounds. *Curr. Med. Chem.* **2016**, *23*, 383–405. [CrossRef] [PubMed]
49. Yu, H.P.; Hsieh, P.W.; Chang, Y.J.; Chung, P.J.; Kuo, L.M.; Hwang, T.L. 2-(2-Fluorobenzamido)benzoate ethyl ester (EFB-1) inhibits superoxide production by human neutrophils and attenuates hemorrhagic shock-induced organ dysfunction in rats. *Free. Radic. Biol. Med.* **2011**, *50*, 1737–1748. [CrossRef] [PubMed]